

DESY 03-051
LU-ITP 2003/006
Edinburgh-2003/04
LTH-573
MIT-CTP-3365

Generalized Parton Distributions from Lattice QCD

M. Göckeler^{1,2}, R. Horsley³, D. Pleiter⁴, P.E.L. Rakow⁵,
A. Schäfer², G. Schierholz^{4,6} and W. Schroers⁷

¹ *Institut für Theoretische Physik, Universität Leipzig, D-04109 Leipzig, Germany*

² *Institut für Theoretische Physik, Universität Regensburg, D-93040 Regensburg, Germany*

³ *School of Physics, University of Edinburgh, Edinburgh EH9 3JZ, UK*

⁴ *John von Neumann-Institut für Computing NIC,
Deutsches Elektronen-Synchrotron DESY, D-15738 Zeuthen, Germany*

⁵ *Theoretical Physics Division, Department of Mathematical Sciences,
University of Liverpool, Liverpool L69 3BX, UK*

⁶ *Deutsches Elektronen-Synchrotron DESY, D-22603 Hamburg, Germany*

⁷ *Center for Theoretical Physics, Massachusetts
Institute of Technology, Cambridge, MA 02139, USA*

- QCDSF Collaboration -

Abstract

We perform a quenched lattice calculation of the first moment of twist-two generalized parton distribution functions of the proton, and assess the total quark (spin and orbital angular momentum) contribution to the spin of the proton.

PACS numbers: 12.38.Gc,13.60.Fz

Generalized parton distributions [1] (GPDs) provide a deeper understanding of the internal structure of hadrons in terms of quarks and gluons. While ordinary parton distributions measure the probability $|\psi(x)|^2$ of finding a parton with fractional momentum x in the hadron, GPDs describe the coherence of two different hadron wave functions $\psi^\dagger(x + \xi/2)\psi(x - \xi/2)$, one where the parton carries fractional momentum $x + \xi/2$ and one where this fraction is $x - \xi/2$, from which information about parton-parton correlation functions can be deduced. As a consequence, GPDs depend on the momentum transfer Δ^2 between the initial and final hadron, which provides further information on the transverse location of quarks and gluons [2]. Spatial images of hadrons can thus be obtained, where the resolution is determined by the virtuality Q^2 of the incoming photon. Last, but not least, GPDs allow us to isolate the contribution of the quark orbital angular momentum to the spin of hadrons. Lattice QCD is the only known method that is able to compute moments of GPDs from first principles.

We will restrict ourselves to the GPDs H_q and E_q of the nucleon, where $q = u, d, \dots$ denotes the flavor of the struck quark. We will not consider the gluon sector here. The lowest, zeroth moments of H_q and E_q are given by the Dirac and Pauli form factors:

$$\int_{-1}^1 dx H_q(x, \xi, \Delta^2) = F_1^q(\Delta^2), \quad (1)$$

$$\int_{-1}^1 dx E_q(x, \xi, \Delta^2) = F_2^q(\Delta^2). \quad (2)$$

Both form factors have been computed on the lattice in a similar calculation [3] to the present one and found to be well described by a dipole ansatz

$$F_{1,2}^q(\Delta^2) = F_{1,2}^q(0)/(1 - \Delta^2/M_{1,2}^2)^2 \quad (3)$$

for sufficiently small (and accessible) momenta, with dipole masses $M_{1,2}$ of the order of the ρ, ω mass, when extrapolated to the physical pion mass.

The first moments of H_q and E_q are of the form [1]

$$\int_{-1}^1 dx x H_q(x, \xi, \Delta^2) = A_2^q(\Delta^2) + \xi^2 C_2^q(\Delta^2), \quad (4)$$

$$\int_{-1}^1 dx x E_q(x, \xi, \Delta^2) = B_2^q(\Delta^2) - \xi^2 C_2^q(\Delta^2), \quad (5)$$

TABLE I: Parameters of the dipole fit. In the bottom row we give the parameters extrapolated to the physical pion mass.

κ	M [GeV]	$A_2^u(0)$	$B_2^u(0)$	$C_2^u(0)$	$A_2^d(0)$	$B_2^d(0)$	$C_2^d(0)$
0.1324	1.69(05)	0.419(07)	0.344(028)	-0.084(26)	0.188(04)	-0.281(20)	-0.071(15)
0.1333	1.58(06)	0.415(10)	0.334(044)	-0.101(35)	0.176(05)	-0.260(29)	-0.073(19)
0.1342	1.41(10)	0.404(19)	0.357(117)	-0.117(70)	0.158(10)	-0.265(80)	-0.067(35)
	1.11(20)	0.400(22)	0.334(113)	-0.134(81)	0.147(11)	-0.232(77)	-0.071(42)

where $A_2^q(\Delta^2)$, $B_2^q(\Delta^2)$ and $C_2^q(\Delta^2)$ are generalized form factors, which are given by the nucleon matrix elements of the energy-momentum tensor (EMT):

$$\begin{aligned}
\langle p' | \mathcal{O}_{\{\mu\nu\}}^q | p \rangle &\equiv \frac{i}{2} \langle p' | \bar{q} \gamma_{\{\mu} \overleftrightarrow{D}_{\nu\}} q | p \rangle \\
&= A_2^q(\Delta^2) \bar{u}(p') \gamma_{\{\mu} \bar{p}_{\nu\}} u(p) \\
&\quad - B_2^q(\Delta^2) \frac{i}{2m_N} \bar{u}(p') \Delta^\alpha \sigma_{\alpha\{\mu} \bar{p}_{\nu\}} u(p) \\
&\quad + C_2^q(\Delta^2) \frac{1}{m_N} \bar{u}(p') u(p) \Delta_{\{\mu} \Delta_{\nu\}}.
\end{aligned} \tag{6}$$

Here m_N denotes the nucleon mass, $\bar{p} = \frac{1}{2}(p' + p)$, $\Delta = p' - p$, and curly brackets refer to symmetrization of indices and subtraction of traces. The EMT has twist two and spin two. It is assumed to be renormalized at the scale μ , which makes $A_2^q(\Delta^2)$, $B_2^q(\Delta^2)$ and $C_2^q(\Delta^2)$ scale and scheme dependent. For the classification of states of definite J^{PC} contributing to (6) in the t -channel see [4]. The so-called skewedness parameter ξ is defined by $\xi = -n \cdot \Delta$, where n is a light-like vector with $n \cdot \bar{p} = 1$, and bounded by $|\xi| \leq 2\sqrt{\Delta^2/(\Delta^2 - 4m_N^2)}$. In the forward limit, $\Delta^2 \rightarrow 0$, we have

$$A_2^q(0) = \langle x_q \rangle \equiv \int_0^1 dx x (q_\uparrow(x) + q_\downarrow(x)), \tag{7}$$

where $q_{\uparrow(\downarrow)}(x)$ are the usual quark distributions with spin parallel (antiparallel) to the spin of the nucleon. Furthermore, one derives [5]

$$\frac{1}{2}(A_2^q(0) + B_2^q(0)) = J_q, \tag{8}$$

where J_q is the angular momentum of the q quark, and $J = \sum_q J_q$ is the total angular momentum of the nucleon carried by the quarks. The angular momentum decomposes, in a

gauge invariant way, into two pieces:

$$J_q = L_q + S_q, \quad (9)$$

where L_q is the orbital angular momentum and

$$S_q = \frac{1}{2}\Delta q \equiv \frac{1}{2} \int_0^1 dx (q_\uparrow(x) - q_\downarrow(x)) \quad (10)$$

is the spin of the quark. We know Δq from separate calculations [6, 7], so that L_q can be computed from (8).

In this Letter we perform a quenched lattice calculation of the generalized form factors $A_2^q(\Delta^2)$, $B_2^q(\Delta^2)$ and $C_2^q(\Delta^2)$. The quenched approximation neglects fluctuations of virtual quark-antiquark pairs from the Dirac sea. The non-forward matrix elements (6) are computed from ratios of three- and two-point functions following [3]. Further details are given in [8]. To keep cut-off effects small, we use non-perturbatively $\mathcal{O}(a)$ improved Wilson fermions. The calculation is done on $16^3 32$ lattices at $\beta = 6.0$ and for three different hopping parameters, $\kappa = 0.1324, 0.1333$ and 0.1342 , which allows us to extrapolate our results to the chiral limit. Using $r_0 = 0.5$ fm to set the scale, which results in the inverse lattice spacing $1/a = 2.12$ GeV, the corresponding pion masses are 1070, 870 and 640 MeV. If we use the nucleon mass extrapolated to the chiral limit to set the scale, the pion masses are 930, 760 and 550 MeV, and $1/a = 1.84$ GeV. The corresponding nucleon masses and the choice of nucleon momenta p, p' can be inferred from [3]. For the EMT we consider two sets of (euclidean) operators:

$$\frac{1}{\sqrt{2}}(\mathcal{O}_{\mu\nu} + \mathcal{O}_{\nu\mu}), \quad 1 \leq \mu < \nu \leq 4 \quad (11)$$

and

$$\begin{aligned} & \frac{1}{2}(\mathcal{O}_{11} + \mathcal{O}_{22} - \mathcal{O}_{33} - \mathcal{O}_{44}), \\ & \frac{1}{\sqrt{2}}(\mathcal{O}_{33} - \mathcal{O}_{44}), \quad \frac{1}{\sqrt{2}}(\mathcal{O}_{11} - \mathcal{O}_{22}). \end{aligned} \quad (12)$$

Each set transforms irreducibly under the hypercubic group. The operators (11) and (12) are renormalized multiplicatively, $\mathcal{O}(\mu) = Z(a\mu) \mathcal{O}(a)$, with renormalization constants [6] $Z_{v_{2a}}$ and $Z_{v_{2b}}$, respectively. The renormalization constants are computed non-perturbatively [9] following [10]. We obtain $Z_{v_{2a}}^{\overline{MS}}(2 \text{ GeV}) = 1.10$ and $Z_{v_{2b}}^{\overline{MS}}(2 \text{ GeV}) = 1.09$. The following results refer to the \overline{MS} scheme at the renormalization scale $\mu = 2$ GeV.

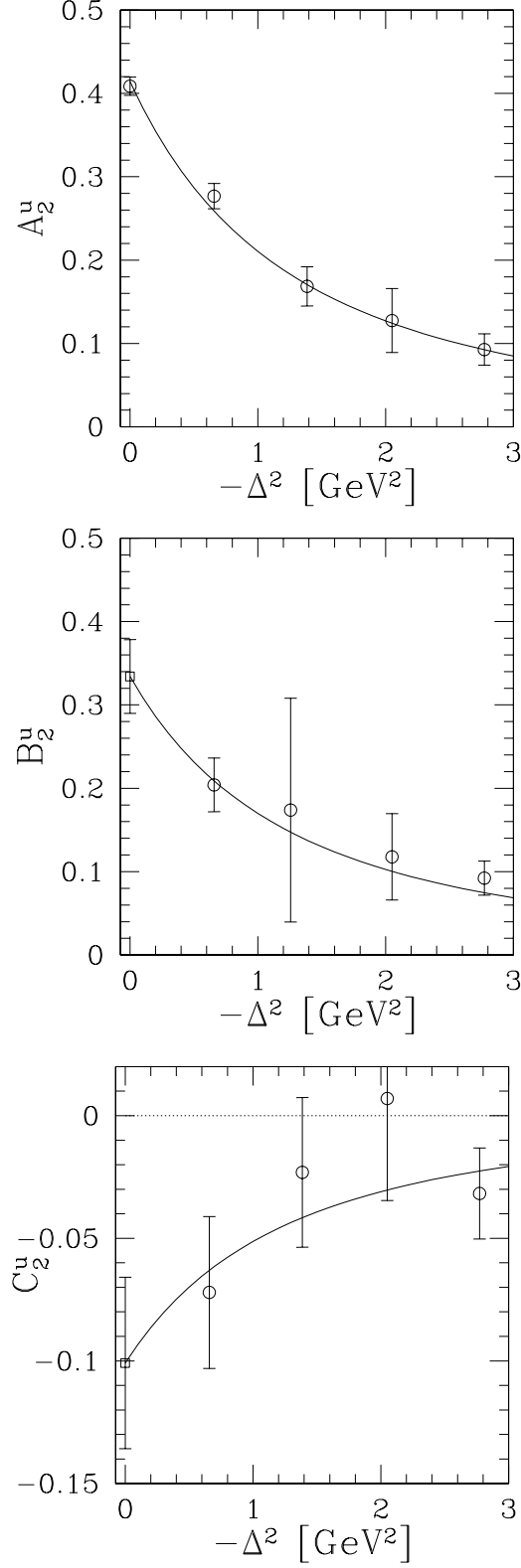


FIG. 1: The generalized form factors A_2^u , B_2^u and C_2^u at $\kappa = 0.1333$, together with the dipole fit and the extrapolated values at $\Delta^2 = 0$ (□).

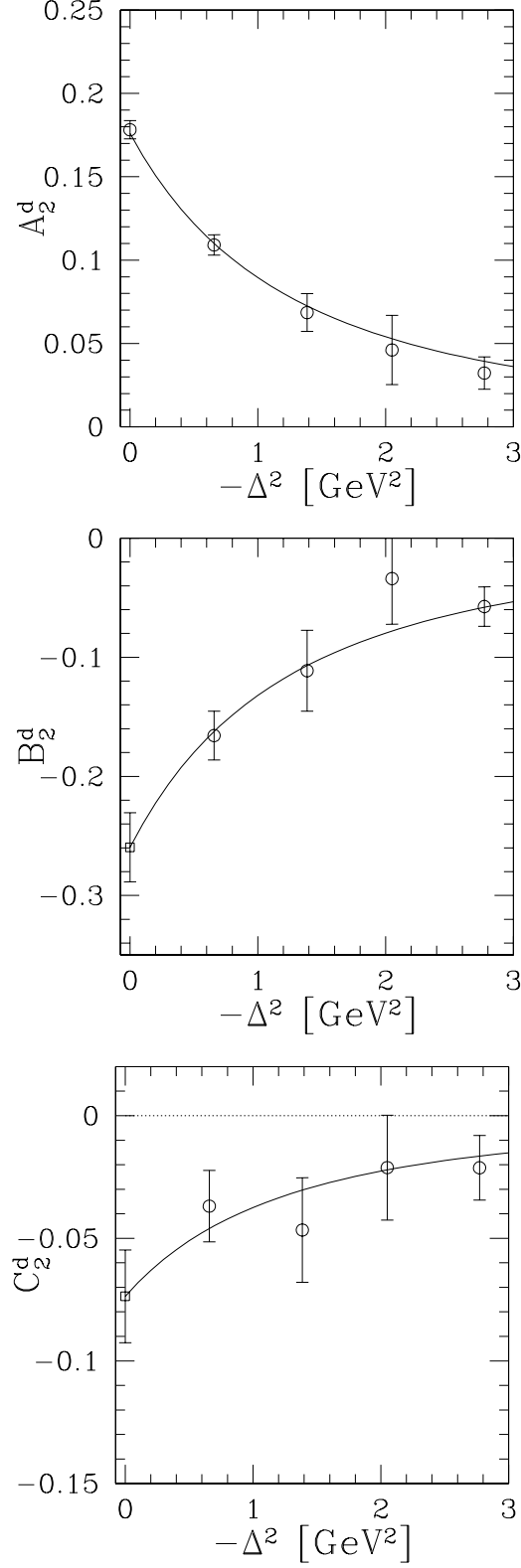


FIG. 2: The generalized form factors A_2^d , B_2^d and C_2^d at $\kappa = 0.1333$, together with the dipole fit and the extrapolated values at $\Delta^2 = 0$ (\square).

In Figs. 1 and 2 we show the generalized form factors $A_2^u(\Delta^2)$, $B_2^u(\Delta^2)$, $C_2^u(\Delta^2)$ and $A_2^d(\Delta^2)$, $B_2^d(\Delta^2)$, $C_2^d(\Delta^2)$ of the proton for $\kappa = 0.1333$. Data points with larger errors are not shown here but are included in the fit. The corresponding form factors of the neutron are obtained by interchanging u and d . Similarly good results are found for $\kappa = 0.1324$ and 0.1342 . The generalized form factors can be well described by the dipole ansatz

$$A_2^q(\Delta^2) = A_2^q(0)/(1 - \Delta^2/M^2)^2, \quad (13)$$

and similarly for B_2^q and C_2^q . Fits of $A_2^u(\Delta^2)$ and $A_2^d(\Delta^2)$ give the same dipole mass M within errors. The dipole masses obtained from separate fits of $B_2^u(\Delta^2)$, $B_2^d(\Delta^2)$, $C_2^u(\Delta^2)$ and $C_2^d(\Delta^2)$ are found to be consistent with that value. We therefore have decided to fit our data by a common dipole mass M . Our data do not favor a monopole behavior. The results of the fits are shown in Table I. For a reliable extrapolation to $\Delta^2 = 0$ we find it important to cover a wide enough range of Δ^2 values. This may be the reason why our dipole masses turn out to be systematically larger than those found in a previous calculation [11].

In Fig. 3 we show the dipole mass M as a function of the pion mass. The mass values appear to lie on a straight line, as was observed already in the case of the nucleon form factors [3]. A linear extrapolation in m_π to the physical pion mass gives $M = 1.1(2)$ GeV. This value is close to the physical masses of the f_2 , a_2 mesons, which supports the hypothesis of tensor meson dominance. A quadratic extrapolation in m_π leads to $M = 1.3(1)$ GeV. The form factor data $A_2^q(0)$, $B_2^q(0)$ and $C_2^q(0)$ show little variation with the quark mass and are extrapolated quadratically in m_π to the physical pion mass. The results are shown in the bottom row of Table I. It should be stressed that all quantities refer (at best) to valence quark distributions, because sea quark effects have been neglected. In unquenched simulations there are also quark-line disconnected contributions. For an estimate see [11].

If the dipole behavior (3), (13) continues to hold for the higher moments as well, and if we assume that the dipole masses continue to grow in a Regge-like fashion, we would obtain

$$\int_{-1}^1 dx x^n H_q(x, 0, \Delta^2) = \langle x_q^n \rangle / (1 - \Delta^2/M_{n+1}^2)^2, \quad (14)$$

with $M_l^2 = \text{const.} + l/\alpha'$, α' being the slope of the Regge trajectory. This would mean that with increasing momentum transfer $|\Delta^2|$ the lower moments of $H_q(x, 0, \Delta^2)$ are suppressed more than the higher ones, so that the observed peak in $H_q(x, 0, 0) = q_\uparrow(x) + q_\downarrow(x)$ around

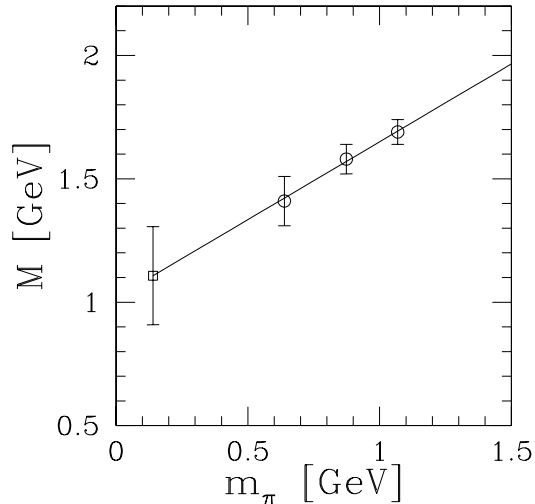


FIG. 3: The dipole mass M as a function of m_π , together with a linear extrapolation to the physical pion mass (\square).

$x \approx 0.2$ is shifted towards the higher values of x . As a result, the Δ^2 dependence cannot be factorized in a simple way, as is sometimes assumed. Knowing $\langle x_q^n \rangle$, we can reconstruct $H_q(x, 0, \Delta^2)$ from (14) by inverse Mellin transform. The ξ dependence of both H_q and E_q appears to be rather weak, based on our knowledge of the first two moments, and in the isovector channel (corresponding to proton–neutron or u – d matrix elements) it largely cancels out.

In Fig. 4 we show the total angular momentum $J = J_u + J_d$. The dependence on the pion mass is rather flat, as expected [12]. The errors are due to the relatively large statistical errors of B_2^u and B_2^d and the fact that B_2^u and B_2^d cancel to a large extent. In Table II we give our results for J , and separately for J_q and S_q , extrapolated quadratically (linearly in m_π^2) to the physical pion mass. The numbers for S_q refer to our latest results [9], computed from the non-perturbatively improved axial vector current with non-perturbative renormalization factors. It turns out that the total angular momentum J carried by the quarks amounts to $\approx 70\%$ of the spin of the (quenched) proton, leaving a contribution of $\approx 30\%$ for the gluons. The major contribution is given by the u quark, while the contribution of the d quark is found to be negligible, which hints at strong pairing effects. Our result for J is somewhat smaller than that of [11, 13]. We are able to compute L_q now. The total orbital angular

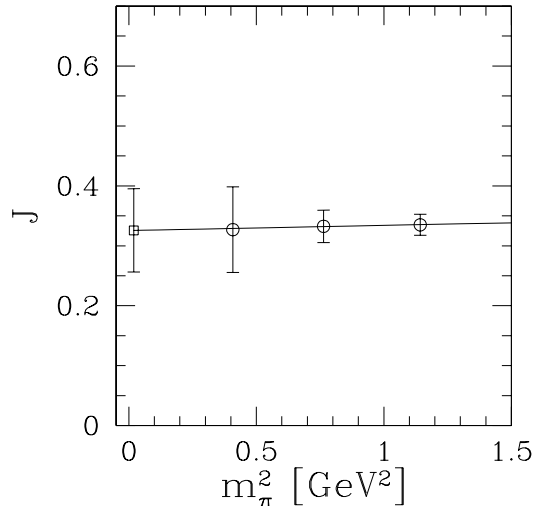


FIG. 4: The total angular momentum J , together with a quadratic extrapolation to the physical pion mass (\square).

TABLE II: The total angular momentum and its individual contributions, extrapolated to the physical pion mass.

J	J_u	J_d	S_u	S_d
0.33(7)	0.37(6)	-0.04(4)	0.42(1)	-0.12(1)

momentum of the quarks turns out to be consistent with zero:

$$L \equiv L_u + L_d = 0.03(7). \quad (15)$$

This indicates that (at virtuality $\mu = 2 \text{ GeV}$) the parton's transverse momentum in the (quenched) proton is small. A similar conclusion can be drawn from our earlier finding [14] of a small twist-three contribution d_2 to the second moment of the polarized structure function g_2 .

The generalized form factors $C_2^q(\Delta^2)$ contribute to the beam charge asymmetry of deeply virtual Compton scattering. We obtain a rather small value: $C_2^u(0) + C_2^d(0) = -0.2(1)$. This result is to be compared with the value -0.8 obtained in the chiral quark-soliton model at $\mu \approx 0.6 \text{ GeV}$ [15]. For a discussion see also [16].

As far as one can compare, quenched and unquenched results agree surprisingly well, and we do not expect to find significant differences here either. For a recent study of quenching

artifacts, as well as cut-off effects, see [17].

This work is supported by DFG and under the Feodor Lynen program. Discussions with P. Hägler, J. Negele, D. Renner and C. Weiss are acknowledged. The numerical calculations have been performed at NIC (Jülich).

-
- [1] D. Müller et al., *Fortsch. Phys.* 42, 101 (1994); X. Ji, *Phys. Rev. Lett.* 78, 610 (1997); A.V. Radyushkin, *Phys. Rev. D* 56, 5524 (1997); M. Diehl et al., *Phys. Lett. B* 411, 193 (1997); X. Ji, *J. Phys. G* 24, 1181 (1998); J. Blümlein, B. Geyer and D. Robaschik, *Nucl. Phys. B* 560, 283 (1999).
 - [2] M. Diehl, *Eur. Phys. J. C* 25, 223 (2002); M. Burkardt, *Int. J. Mod. Phys. A* 18, 173 (2003).
 - [3] M. Göckeler et al., [hep-lat/0303019](#).
 - [4] X. Ji and R.F. Lebed, *Phys. Rev. D* 63, 076005 (2001).
 - [5] X. Ji, *Phys. Rev. Lett.* 78, 610 (1997).
 - [6] M. Göckeler et al., *Phys. Rev. D* 53, 2317 (1996).
 - [7] M. Fukugita et al., *Phys. Rev. Lett.* 75, 2092 (1995); S.J. Dong, J.-F. Lagaë and K.F. Liu, *Phys. Rev. Lett.* 75, 2096 (1995); S. Capitani et al., *Nucl. Phys. (Proc. Suppl.)* 79, 548 (1999); S. Güsken et al., *Phys. Rev. D* 59, 114502 (1999); D. Dolgov et al., *Phys. Rev. D* 66, 034506 (2002).
 - [8] P. Hägler et al., [hep-lat/0304018](#).
 - [9] M. Göckeler et al., in preparation.
 - [10] G. Martinelli et al., *Nucl. Phys. B* 445, 81 (1995); M. Göckeler et al., *Nucl. Phys. B* 544, 699 (1999).
 - [11] N. Mathur et al., *Phys. Rev. D* 62, 114504 (2000).
 - [12] J.-W. Chen and X. Ji, *Phys. Rev. Lett.* 88, 052003 (2002).
 - [13] V. Gadiyak, X. Ji and C. Jung, *Phys. Rev. D* 65, 094510 (2002); see however: W. Wilcox, *Phys. Rev. D* 66, 017502 (2002).
 - [14] M. Göckeler et al., *Phys. Rev. D* 63, 074506 (2001).
 - [15] N. Kivel, M.V. Polyakov and M. Vanderhaeghen, *Phys. Rev. D* 63, 114014 (2001); V.Yu. Petrov et al., *Phys. Rev. D* 57, 4325 (1998).

- [16] A.V. Belitsky and D. Müller, Nucl. Phys. A711, 118 (2002); F. Ellinghaus, Nucl. Phys. A711, 171 (2002); A. Freund, M. McDermott and M. Strikman, Phys. Rev. D67, 036001 (2003).
- [17] T. Bakeyev et al., [hep-lat/0311017](#).